Available online at www.sciencedirect.com

SCIENCE DIRECT®

NUCLEAR SCIENCE AND TECHNIQUES

Nuclear Science and Techniques, Vol.17, No.5 (2006) 301–307

# The development and verification of thermal-hydraulic code on passive residual heat removal system of Chinese advanced PWR

XIAO Ze-Jun[1,2,*] QIU Sui-Zheng[2] ZHUO Wen-Bin[1] FAN Pu[2] CHEN Bing-De[1] JIA Dou-Nan[2]

([1]National Key Laboratory of Bubble Physics & Natural Circulation, Nuclear Power Institute of China, Chengdu 610041, China;

[2]Xi'an Jiaotong University, Xi'an, 710049, China)

**Abstract** The technology of passive safety is the current trend among safety systems in nuclear power plant. Passive residual heat removal system (PRHRS), a major part of passive safety systems of Chinese advanced PWR, is a novel design with three-fold natural circulation. On the basis of reasonable physics and mathematics models, MITAP-PRHRS code was developed to analyze steady and transient characteristics of the PRHRS. The calculation and analysis show that the code simulates steady characteristics of the PRHRS very well, and it is able to simulate transient characteristics of all startup modes of the PRHRS. However, the quantitative description is poor during the initial stages of the transition process when water hammer occurs.

**Key words** Chinese advanced PWR, Passive residual heat removal system, Thermal-hydraulic code

**CLC numbers** TL361, TK222

## 1 Introduction

The technology of passive safety is the trend of safety systems in nuclear power plant, and various novel reactor concepts, including AP600, EPP1000, SPWR, WWER1000, and MS600, have adopted passive safety systems [1]. Passive safety system is one of the main features of Chinese advanced PWR, which is different from other conventional PWR [2]. Passive residual heat removal system (PRHRS), which accounts for the majority of passive safety systems of Chinese advanced PWR, is a novel design with three-fold natural circulation (Fig.1). It consists of three loops: (1) reactor coolant system by which the decay heat is transferred to the secondary side of steam generator; (2) steam water loop including steam generator (SG), air cooler, and emergency feed water tank (EFWT); and (3) air loop. The principle of working of PRHRS is as follows. When blackout or other accident occurs, the isolation valves located at the outlet pipe of emergency feed water tank (EFWT) is opened by a low-low water signal for the SG, so that EFWT provides water to the secondary side of SG by gravity and maintains the water level. The water in the SG absorbs the residual heat during its transformation into steam. The steam that rises and passes through the air cooler condenses into water in the air cooler. Simultaneously, the heat is transferred to the air through the natural convection of air occurring in chimney and in atmosphere. And then, the condensed water returns to the SG loop by gravity, thereby establishing a continuous natural circulation flow. On the basis of reasonable physical and mathematical models, MITAP-PRHRS code was developed to analyze steady and transient characteristic of the PRHRS. In this article, the development and verification of MITAP-PRHRS code are introduced.

*E-mail: xzj670711@vip.sina.com

Received date: 2005-12-16

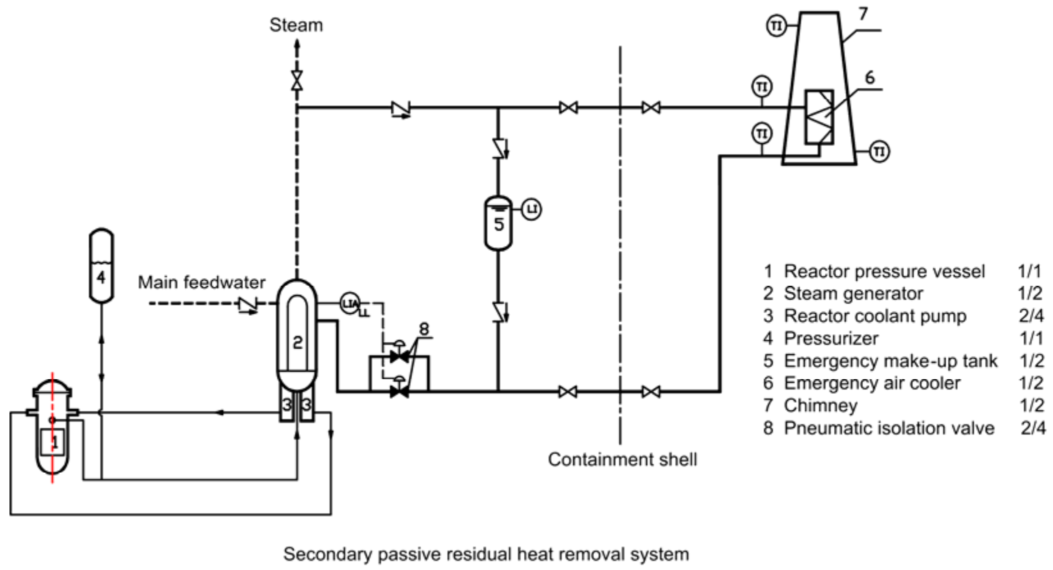


**Fig. 1** Schematic diagram of the PRHRS.

## 2 Mathematical model

Control volume of the PRHRS is shown in Fig.2. Basic assumptions are as follows：(1) the model is one dimensional, (2) incompressible flow, (3) neglecting the gravitational work and the work related to the kinetic energy, and (4) adiabatic flow for pipe and plenum.

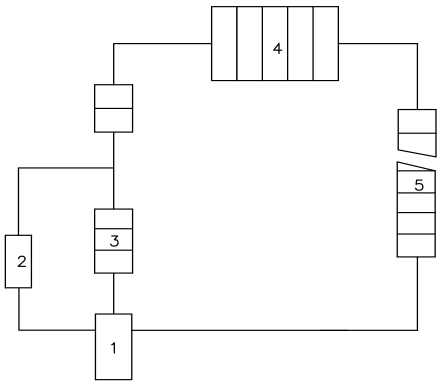


1-SG, 2-EFWT, 3-Upward section, 4-Air cooler, 5-Downward section.

**Fig. 2** Schematic diagram of control volume for the PRHRS.

### 2.1 Single-phase conservative equations

Single-phase conservative equations are applied in primary side and the downcomer of SG, secondary-side subcooling section of SG, upward section and downward section of the PRHRS, etc. Mass conservation equation, momentum balance equation, and energy conservation equation are listed as follows:

$$\frac{\partial \rho}{\partial \tau}+\frac{1}{A}\frac{\mathrm{d}W}{\mathrm{d}Z}=0 \tag{1}$$

$$\frac{\partial W}{\partial \tau}+\frac{\partial}{\partial Z}\left(\frac{W^2}{\rho A}\right)=-A\frac{\partial P}{\partial Z}-\int_{U_\mathrm{w}}\tau_f\,\mathrm{d}U-\rho g A \tag{2}$$

$$\rho\frac{\partial h}{\partial \tau}+\frac{W}{A}\frac{\partial h}{\partial Z}=\frac{qU_\mathrm{h}}{A}+\frac{\partial P}{\partial \tau} \tag{3}$$

where $W$, $\rho$, $A$, $P$, $h$, $U_\mathrm{w}$, $U_\mathrm{h}$, $\tau_f$, and $q$ represent flow rate, fluid density, the cross-sectional area of flow channel, system pressure, enthalpy, wetted perimeter, heated perimeter, shear stress at the wall, and heat flux, respectively.

### 2.2 Two-phase mixture conservative equations

Two-phase mixture conservative equations are applied in secondary-side boiling section of SG, mixture of air cooler, etc. Mixture mass conservation equation, mixture momentum balance equation, and mixture energy conservation equation are listed as follows:

$$\frac{\partial}{\partial \tau}\left[(1-\alpha)\rho_\mathrm{f}+\alpha\rho_\mathrm{g}\right]+\frac{\partial}{\partial Z}\left[(1-\alpha)\rho_\mathrm{f}V_\mathrm{f}+\alpha\rho_\mathrm{g}V_\mathrm{g}\right]=0 \tag{4}$$

$$\frac{\partial W}{\partial \tau}=-A\frac{\partial P}{\partial Z}-\int_{U_\mathrm{w}}\tau_f\mathrm{d}l-\rho g A-\frac{\partial}{\partial Z}\left(\frac{W^2}{\rho A}\right) \tag{5}$$

$$\frac{\partial}{\partial\tau}\left[\left(1-\alpha\right)\rho_{\mathrm{f}}h_{\mathrm{f}}+\alpha\rho_{\mathrm{g}}h_{\mathrm{g}}\right]+\frac{1}{A}\frac{\partial}{\partial Z}\left[Wh\right]=\frac{qU_{\mathrm{h}}}{A}+\frac{\partial P}{\partial\tau} \quad (6)$$

where $\alpha$ represents void fraction, and subscripts g and f represent steam and saturated water, respectively.

### 2.3 The wall temperature equation of U tube for SG and air cooler

The wall temperature equation of U tube for SG and air cooler is as follows:

$$M_{\mathrm{U}}Cp_{\mathrm{U}}\frac{\partial T_{\mathrm{U}}\left(\tau\right)}{\partial\tau}= \alpha_{\mathrm{U_1}}F_{\mathrm{U_1}}\left(T_{\mathrm{U_1}}-T_{\mathrm{WU}}\right)-\alpha_{\mathrm{U_2}}F_{\mathrm{U_2}}\left(T_{\mathrm{WU}}-T_{\mathrm{U_2}}\right) \quad (7)$$

where $M$, $C$p, $F$, and $T$ represent mass, specific heat, heat transfer area, and temperature, respectively; subscript U represents either U tube or ribbed tube of air cooler; subscript WU represents wall of either U tube or ribbed tube of air cooler; subscripts $U_1$ and $U_2$ represent primary side and secondary side of each SG or air cooler, respectively.

### 2.4 The water level equation of SG and the enthalpy equation of the downcomer

SG (Fig.3) consists of U-tube, steam dome, feed water dome, downcomer, riser section, and lower plenum. The water level equation of SG [3-5] is as follows:

$$\frac{\partial L}{\partial\tau}= \frac{W_{\mathrm{fw}}+W_{\mathrm{afw}}-X_{\mathrm{RIR}}W_{\mathrm{S}}}{A_{\mathrm{dc}}\rho_{\mathrm{dc}}}-\frac{L}{\rho_{\mathrm{dc}}}\left(\frac{\partial\rho_{\mathrm{dc}}}{\partial p}\frac{\partial p}{\partial\tau}+\frac{\partial\rho_{\mathrm{dc}}}{\partial h_{\mathrm{dc}}}\cdot\frac{\partial h_{\mathrm{dc}}}{\partial\tau}\right) \quad (8)$$

where $L$, $X_{RIR}$, and $W_S$ represent water level, outlet quality of riser section, and secondary side circulation flow rate of SG, respectively; subscripts afw, dc, and fw represent emergency feed water, downcomer, and feed water, respectively.

The enthalpy equation of the downcomer is as follows:

$$\frac{\partial h_{\mathrm{dc}}}{\partial\tau}=\frac{[(1-X_{\mathrm{RIR}})W_{\mathrm{S}}h_{\mathrm{f}}+W_{\mathrm{fw}}h_{\mathrm{fw}}+W_{\mathrm{afw}}h_{\mathrm{afw}}-W_{\mathrm{S}}h_{\mathrm{dc}}]}{(A_{\mathrm{dc}}\rho_{\mathrm{dc}}L)}- \frac{(W_{\mathrm{fw}}+W_{\mathrm{afw}}-X_{\mathrm{RIR}}W_{\mathrm{S}})h_{\mathrm{dc}}}{(A_{\mathrm{dc}}\rho_{\mathrm{dc}}L)} \quad (9)$$

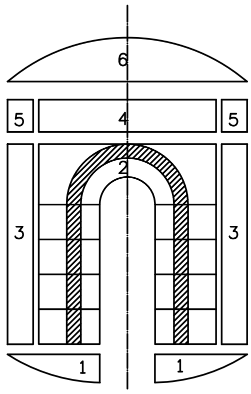


1 – Lower plenum, 2 – U-tube, 3 – Downcomer, 4 – Riser section, 5 – Feed water dome, 6 – Steam dome.

**Fig. 3** Schematic diagram of control volume for SG.

### 2.5 The pressure equation of SG

The pressure equation of SG is as follows:

$$\frac{\partial P}{\partial\tau}=\frac{F-E}{G} \quad (10)$$

where $E=V_{\mathrm{RIR}}(\rho_{\mathrm{g}}h_{\mathrm{g}}-\rho_{\mathrm{f}}h_{\mathrm{f}})\frac{\partial\alpha_{\mathrm{RIR}}}{\partial\tau}$

$$F=h_{\mathrm{g}}(W_{\mathrm{go}}-W_{\mathrm{STM}}-W_{\mathrm{V}})$$

$$G=(V_{\mathrm{SD}}+\alpha_{\mathrm{RIR}}V_{\mathrm{RIR}})\left(\frac{\partial\rho_{\mathrm{g}}}{\partial P}h_{\mathrm{g}}+\rho_{\mathrm{g}}\frac{\partial h_{\mathrm{g}}}{\partial P}-1\right)+ [V_{\mathrm{UPFWR}}+V_{\mathrm{RIR}}(1-\alpha_{\mathrm{RIR}})]\left(\frac{\partial\rho_{\mathrm{f}}}{\partial P}h_{\mathrm{f}}+\rho_{\mathrm{f}}\frac{\partial h_{\mathrm{f}}}{\partial P}\right)$$

where $\alpha_{RIR}$, $V_{RIR}$, $V_{SD}$, $V_{UPFWR}$, $W_{go}$, $W_{STM}$, and $W_V$ represent outlet void fraction of riser section, volume of riser section, volume of steam dome, upper volume of feed water ring with J-tube, steam flow rate of riser section, outlet steam flow rate of riser section for SG, and relieved flow rate through safety valve, respectively.

### 2.6 Void fraction equation of SG

Void fraction equation of SG is as follows:

$$\frac{\partial\alpha_{\mathrm{RIR}}}{\partial\tau}=W_{\mathrm{S}}\left(X_{\mathrm{RIR}}-X_{\mathrm{out}}\right)\Big/\left(V_{\mathrm{RIR}}\rho_{\mathrm{g}}\right) \quad (11)$$

where $X_{out}$ represents outlet quality in SG heating section.

### 2.7 Natural circulation flow-rate equation of the PRHRS and secondary-side circulation flow rate of SG

Natural circulation flow-rate equation of the

PRHRS and secondary-side circulation flow rate of SG is as follows:

$$\frac{\partial W}{\partial \tau}=\frac{-\oint \rho g \,\mathrm{d} z-\oint \frac{U_{\mathrm{w}} f_{\mathrm{w}} W^{2}}{2 \rho A^{3}} \mathrm{d} z-W^{2} \sum_{i} \frac{K_{\mathrm{loc}}}{2 \rho_{i} A_{i}^{2}}}{\oint \frac{1}{A} \mathrm{d} z} \quad (12)$$

where $f_{\mathrm{w}}$ and $K_{\mathrm{loc}}$ represent the fanning friction factor and form loss coefficient, respectively; and subscript $i$ represents the control volume.

### 2.8 Natural circulation flow-rate equation of air loop

Natural circulation flow-rate equation of air loop is as follows:

$$\frac{\partial W}{\partial \tau} \int_{0}^{L_{\mathrm{ch}}} \frac{1}{A} \mathrm{d} z = -G^{2}\left(\frac{1}{\rho_{\mathrm{cho}}}-\frac{1}{\rho_{\mathrm{chi}}}\right)-\int_{0}^{L_{\mathrm{ch}}} \rho g \,\mathrm{d} z-W^{2} \int_{0}^{L_{\mathrm{ch}}} \frac{U_{\mathrm{w}}}{A} f_{\mathrm{w}} \frac{1}{2 \rho A^{2}} \mathrm{d} z \quad (13)$$

where $L_{\mathrm{ch}}$ represents the chimney height, subscripts cho and chi represent the chimney outlet and the chimney inlet, respectively.

### 2.9 Pipe and plenum model

Pipe and plenum model is as follows:

$$M \frac{\mathrm{d} h}{\mathrm{d} \tau}=W\left(h_{\mathrm{in}}-h_{\mathrm{out}}\right) \quad (14)$$

where $M$, $h_{\mathrm{in}}$, and $h_{\mathrm{out}}$ represent mass in the control volume, inlet enthalpy in the control volume, and outlet enthalpy in the control volume, respectively.

### 2.10 Thermal-hydraulic correlations

Considering the length limit of the article, thermal-hydraulic correlations consisting of heat-transfer correlations and pressure-drop correlations are omitted here. They can be referred to in Ref. [6].

## 3 Numerical method

Because the three-fold natural circulation systems closely couple with each other, the three-fold natural circulation systems are solved together. After the discretization of the spatial derivative terms in the equations, the following ordinary differential equations are obtained:

$$\frac{\mathrm{d} \vec{y}}{\mathrm{d} t}=\vec{f}\left(t, \vec{y}, \vec{y}'\right) \quad (15)$$

$$\vec{y}(t_{0})=\vec{y}_{0} \quad (16)$$

Therefore, the dynamic simulation of the whole system can be solved as an initial value problem [7]. For the stiff system of differential equations, Gear's algorithm is used traditionally. In this article, Gear's algorithm is used to solve differential equations of the PRHRS.

## 4 Verification of steady characteristics

### 4.1 Steady calculation

According to system characteristics on PRHRS of Chinese advanced PWR, while system pressure, height between heat resource and heat sink, heating power and system resistance are definite, steady characteristics are also definite. Based on steady characteristics, steady calculation has been performed using MITAP-PRHRS code, and influences of some important factors such as system pressure, height between heat resource and heat sink, air inlet temperature, and heating power, on the steady characteristics have been analyzed. A comparison of thresholds of height between heat source and heat sink between MITAP-PRHRS and the correlation [8] has also been made. Steady calculations show that MITAP-PRHRS code can simulate the steady test very well, and relative errors between calculation results and experimental ones were less than $\pm 10\%$, as shown in Tables 1 and 2.

### 4.2 Code application

In the calculation, effects of chimney height and temperature of air at the inlet on steady characteristic of the PRHRS are estimated. As shown in Fig.4, residual heat removal capability is increased as chimney height increases. However, the change is remarkable as chimney height is 8.8—14.8 m, the change is very slow as chimney height is 14.8—18.8m, and change is hardly observed as chimney height is 18.8—20.8m.

**Table 1** Comparison of results of steady state between calculation and test

| Runs | | Pressure /MPa | Height between heat source and heat sink / m | Air inlet temperature / °C | Heating power / kW | Natural circulation flow rate / $kg \cdot h^{-1}$ | Outlet temperature of air cooler / °C | Wind flow rate / $kg \cdot s^{-1}$ | Outlet temperature of chimney /°C |
|---|---|---|---|---|---|---|---|---|---|
| 1 | Test | 3.71 | 6.41 | 31 | 90.5 | 151.3 | 226.1 | 0.56 | 157.5 |
| | Calculation | 3.89 | 6.41 | 31 | 86 | 160.5 | 209.1 | 0.6 | 172.4 |
| 2 | Test | 4.18 | 6.42 | 29.9 | 80.3 | 162.7 | 228.1 | 0.57 | 161.2 |
| | Calculation | 4.1 | 6.42 | 29.9 | 88.5 | 172.3 | 221.2 | 0.6 | 175.5 |
| 3 | Test | 4.66 | 6.4 | 33 | 90 | 158.2 | 210 | 0.56 | 167.9 |
| | Calculation | 4.74 | 6.4 | 33 | 89.1 | 169.8 | 211.3 | 0.6 | 180.6 |
| 4 | Test | 5.31 | 7.03 | 31 | 99.4 | 184.9 | 252.5 | 0.57 | 170.7 |
| | Calculation | 5.47 | 7.04 | 31 | 95.6 | 189.2 | 227 | 0.61 | 187.7 |
| 5 | Test | 6.7 | 6.22 | 35.4 | 99.7 | 179 | 198.1 | 0.58 | 184.5 |
| | Calculation | 6.72 | 6.22 | 35.4 | 94 | 187.5 | 226.8 | 0.6 | 190.6 |
| 6 | Test | 6.7 | 6.24 | 32 | 101.3 | 184 | 218.5 | 0.58 | 184.3 |
| | Calculation | 6.7 | 6.24 | 32 | 100 | 194.6 | 218.3 | 0.6 | 184.1 |
| 7 | Test | 6.7 | 6.24 | 32.3 | 97.3 | 165.8 | 194.9 | 0.58 | 185.5 |
| | Calculation | 6.66 | 6.25 | 32.3 | 95 | 183.4 | 216.9 | 0.59 | 177.6 |
| 8 | Test | 6.7 | 7.05 | 32.6 | 99.8 | 198.8 | 255.2 | 0.58 | 181.2 |
| | Calculation | 6.78 | 7.03 | 32.6 | 104 | 219.9 | 249.6 | 0.61 | 202.1 |
| 9 | Test | 6.7 | 6.24 | 32 | 94.6 | 164.6 | 229.3 | 0.52 | 193 |
| | Calculation | 6.68 | 6.28 | 32 | 86.2 | 180.6 | 246.3 | 0.55 | 188.6 |
| 10 | Test | 6.81 | 6.28 | 34.5 | 81 | 105 | 111.7 | 0.54 | 190.7 |
| | Calculation | 6.88 | 6.33 | 34.5 | 80 | 114.9 | 83.1 | 0.53 | 118.4 |

**Table 2** Comparison of threshold of height between heat source and heat sink between MITAP and correlation

| Runs | Pressure / MPa | SG water level / m | Natural circulation flow rate / $kg \cdot h^{-1}$ | Natural circulation heating power / kW | Threshold of height between heat source and heat sink | |
|---|---|---|---|---|---|---|
| | | | | | Calculation through MITAP / m | Calculation through correlation / m |
| 1 | 7.03 | 6.26 | 146.1 | 61.2 | 5.45 | 5.78 |
| 2 | 6.58 | 6.73 | 159.3 | 68.8 | 6.25 | 6.42 |
| 3 | 7.10 | 6.77 | 188.6 | 78.8 | 7.09 | 7.66 |
| 4 | 6.85 | 6.70 | 194.7 | 82.1 | 8.23 | 7.94 |
| 5 | 6.71 | 6.76 | 233.8 | 99.2 | 9.70 | 9.73 |
| 6 | 5.25 | 5.55 | 261.6 | 118.0 | 10.80 | 11.25 |
| 7 | 5.80 | 5.40 | 272.9 | 120.3 | 11.88 | 11.68 |
| 8 | 7.09 | 5.63 | 294.7 | 123.0 | 12.76 | 12.51 |
| 9 | 6.80 | 5.63 | 311.1 | 131.8 | 13.76 | 13.36 |
| 10 | 6.48 | 5.65 | 335.8 | 143.8 | 14.75 | 14.54 |

Residual heat removal capability is limited if chimney height is too less, but it is meaningless for a residual heat removal system to have a too high chimney. So a suitable chimney height must be considered in engineering design.

As shown in Fig. 5, the driving force of natural circulation is decreased as air inlet temperature is increased, because density difference of air between inlet and outlet is decreased. Therefore, residual heat removal capability is decreased as air inlet temperature is increased.

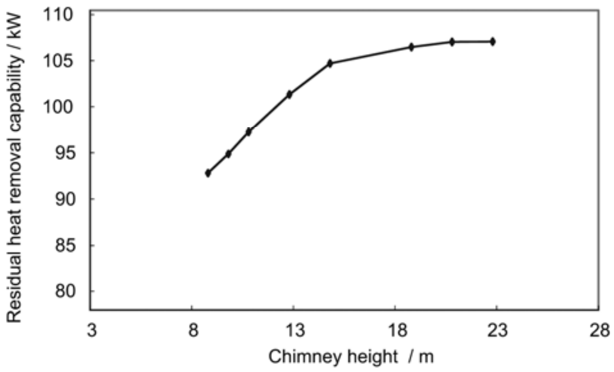


**Fig. 4** Residual heat removal capability vs chimney height.

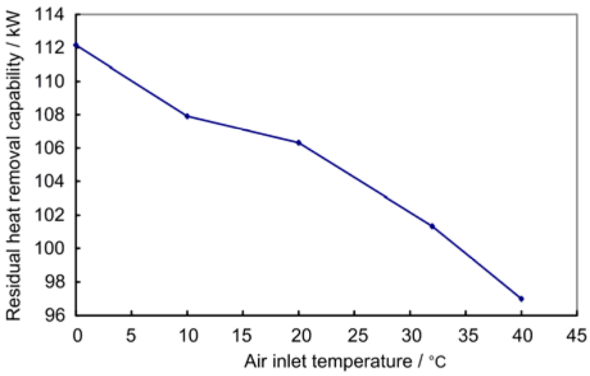


**Fig. 5** Residual heat removal capability vs air inlet temperature.

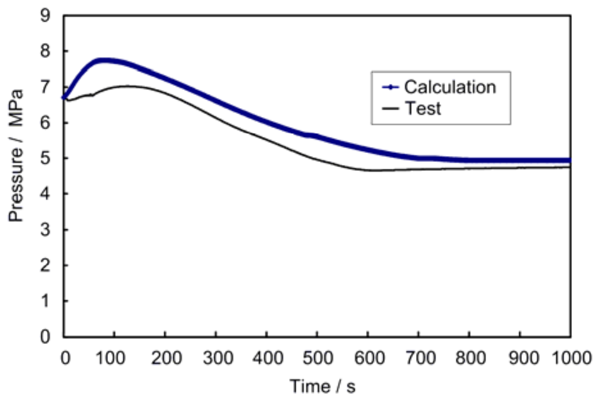


**Fig. 7** Change of pressure with time.

## 5 Verification of transient characteristics

### 5.1 Transient calculation

Transient calculation has been performed using MITAP-PRHRS code, and the transient characteristics were analyzed. Changes of mass flow rate of natural circulation and system pressure with time were calculated and tested, as shown in Figs. 6 and 7. Transient calculations show that MITAP-PRHRS code is able to simulate the transient characteristics of all startup modes [9]. However, the quantitative description is poor during the initial stages of the transition process when water hammer occurs because of the lack of a mechanistic model regarding steam condensation in both emergency feed water tank and air cooler.

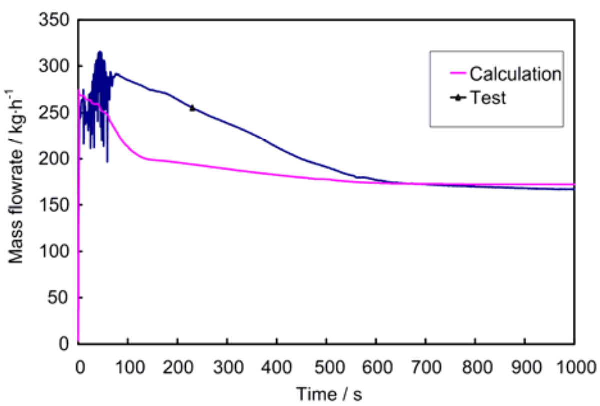


**Fig. 6** Change of mass flow rate of natural circulation with time.

### 5.2 Code application

Effects of chimney height and air temperature at the inlet on transient characteristic of the PRHRS are calculated. As shown in Figs. 8 and 9, the system pressure maximum is decreased as chimney height is increased. Meanwhile, the flow rate maximum is increased, and time is shorter as both system pressure and flow rate reach the maximum.

As shown in Figs. 10 and 11, the system pressure maximum is decreased as air inlet temperature is decreased. Meanwhile, the flow rate maximum is increased, and time for both system pressure and flow rate to reach the maximum is shorter.

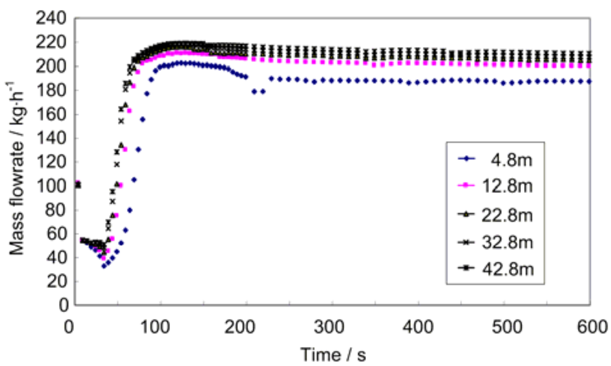


**Fig. 8** Change of mass flow rate of natural circulation with time for different chimney heights.

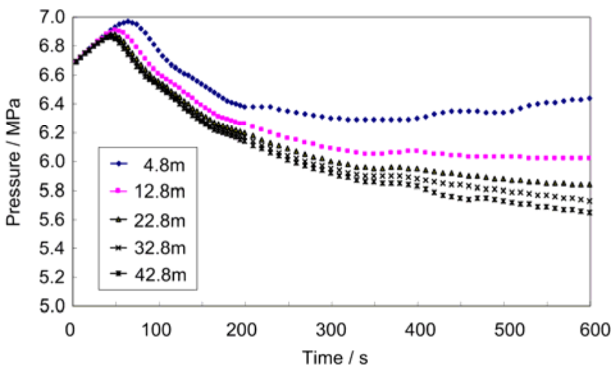


**Fig. 9** Change of pressure with time for different chimney heights.

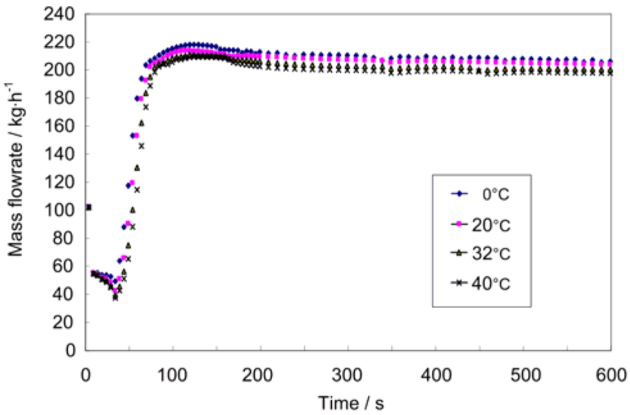


**Fig. 10** Change of mass flow rate of natural circulation with time at different air inlet temperatures.

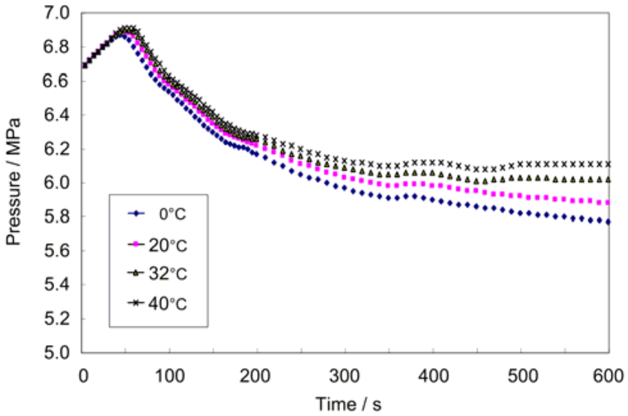


**Fig. 11** Change of pressure with time at different air inlet temperatures.

## 6 Conclusions

On the basis of reasonable physical and mathematical models, MITAP-PRHRS code was developed. MITAP-PRHRS code is a typical code that is used to analyze steady and transient performance of the PRHRS. The calculation and analysis show that the code simulates steady characteristics of the PRHRS very well, and it is able to simulate transient characteristics of all startup modes of the PRHRS. However, the quantitative description is poor in the initial stages of the transition process while water hammer occurs.

MITAP-PRHRS code is an important tool for fulfilling various design tasks of the PRHRS, such as determining system arrangement, equipment capacity, and system startup mode. After it is verified and perfected by test data from new generation 1000MWe PWR PRHRS integrated facility, the MITAP-PRHRS code with self-reliance copyright will be directly used for engineering design of the PRHRS.

## References

1 Juhn P E, Kupitz J, Cleveland J, *et al*. Nuclear Eng. Des., 2000, **201**:41 – 59.

2 Xiao Zejun, Zhuo Wenbin, Zheng Hua, *et al*. Nucl. Eng. Des., 2003, **225**: 305-313.

3 Qiu Suizheng, Zhou Tao, Guo Yujun, *et al*. Nuclear Power Engineering(in Chinese), 1999, **20**: 142-147.

4 Hold A. Nuclear Technology, 1990, **90**:98-118.

5 Arwood D C, Kerlin T W. Nuclear Technology, 1977, **35**: 12-32.

6 Xiao Zejun. Characteristic research on passive residual heat removal system of Chinese advanced PWR. Doctor degree dissertation, Xi'an Jiaotong University. 2004

7 Zang Xinian, Guo Weijun, Huang Bing, *et al*. Nucl. Eng. Des., 2001, **206**:105-111.

8 Xiao Zejun, Zhuo Wenbin, Chen Bingde, *et al*. Nuclear Power Engineering(in Chinese), 2005, **26**:436-442.

9 Xiao Zejun, Zhuo Wenbin, Chen Bingde, *et al*. Nuclear Power Engineering(in Chinese), 2005, **26**: 548-553.